Trans. JWRI, Vol. 25(1996), No.2

Computer Simulation of Thin Sheet Gas-Metal-Arc-Welding

by Prof. Dr.-Ing. Ulrich Dilthey and Dipl.-Ing. Sabine Roosen

ISF Welding Institute, Aachen University, Germany

Abstract

Calculation models included in simulation programs are contributing substantially towards the completion of empirically determined knowledge Calculation models are presented which analyse electrical, thermodynamical and hydrodynamical effects on the GMA-welding process. These models are used in a simulation program for thin sheet GMA-welding process. The MAGSIM program simulates the GMA-welding process calculating the weld shape and the thermo cycle at various points. A graphical display of the cross sections of shape and seam and a three-dimensional view visualise the simulation results. All calculations are available as number values too. The result is rated according to the European Standard EN 25817. Other objectives allow the statistical prediction of quality at welding parameters with tolerances. The automated look for optimised welding parameters for a specific welding task is possible as well.

1. Introduction

The GMA-welding process is, for usual practical welding tasks, described rather well due to experimentally achieved data[1] the opti-misation of weld parameters and weld shape, however, is time- and cost-consuming. By means of a statistical analysis of the empirically achieved data, there is a possibility to optimise parameters and to predict the weld shape. This method, however, works only in determined valid boundaries[2-4]. In addition, the equations of correlations normally content no information about important details like contact-tube distance, length of hose assembly, characteristic of power source, dimensions of the gap, and so on. Another cause for the non-exact reproducibility of such predictions are the neglected influences of the chosen measuring methods, e.g. the location of voltage measuring points.

2. Numerical Simulation of Gas Metal Arc Welding Process

A simulation of the weld formation under consideration of all influences would considerably diminish the efforts for the determination of suitable process parameters, and, in addition, non-experts would also be able to produce solutions for specific welding tasks by means of a computer dialogue. To achieve a detailed description of the weld formation which is also in accordance to the process mechanisms, extensive mathematical models would be necessary, which, however, can only be solved by numerical methods.

Here, the TIG-welding process can be easiest described by a mathematical model[5-7]. Engelst[8] described an arc model which uses experimental data and also takes into account the electromagnetic gasdynamic[9] includes a two-dimensional model of the metal-inertgas-

Transactions of JWRI is published by Joining and Welding Research Institute of Osaka University, Ibaraki, Osaka567, Japan.

spotwelding process where the (classical) normally distributed heat flow density of the arc is widened by the heat flow density of the electrode drop (by empirically found data[10, 11]). [12] describes the numerical simulation of the metal-inertgas-welding process where the average drop temperature (2000°C) is assumed to be the temperature of the weld pool during the V-weld preparation. Pardo and Weckmann[13] introduce a three-dimensional numerical model of the metal-active-gas-weld process by means of which the weld shape can be modeled. The convection of the liquid weld pool is being considered by an increased anisotropic heat conductivity. This method allows the description of the so-called finger penetration. The heat of the drops was taken from theoretical data[14]. To sum up, it can be said that the following topics are not being taken into account:

- connections between electro thermal processes in a consumable electrode, which characterise the distribution of arc and drop heat
- connections between the weld parameters and the arc characteristics (efficiency, effective radius for arc and drop)
- the role of the gap during work piece heating
- generation of weld imperfections, for example, undercuts and burn-through.

The objective of the presented work is the development of a model for the calculation of the GMA-welding process. With this model, practise-oriented boundary conditions should be used, starting from the determination of important welding parameters right to the estimation of the joint in accordance to DIN EN 25817. The basic model of the fusion welding of thin sheets[7] was increased by the description of the GMA arc with consumable electrodes, taking into account the influence of the gap at the heating of the workpiece, the simulation of a possible backing and other details.

2.1 Electrothermal Processes in a Melted Off Electrode and the Appropriate UI-Diagram

The amount of heat brought in the weld pool by the melted wire, in addition to the arc heat, substantially influences welding quality. The objective of the arc description in GMA-welding is the calculation of the thermal power inside the workpiece. The amount of the electrode material put into the work is being considered in the mass balance. To determine the power characteristic of the arc it is necessary to look at the arc model first, **Fig. 1.**

The terms arc voltage, weld voltage and operating voltage are defined differently. The arc voltage ULB is defined as

$$U_{LB} = U_A + U_K + E \cdot Z_{LB} \qquad (1)$$

with U_A anode voltage drop, U_K cathode voltage drop, E arc stream gradient, Z_{LB} length of the arc column. The operating voltage is the voltage, which can be read at the cross of the power source characteristic and the characteristic of the arc in the UI-diagram. It is valid:

$$U_O - I_S \cdot R_q = U_{LB} + I_S(R_{Dr} + R_{KD}) + U_V = U_S + U_V \qquad (2)$$

with U_0 open-circuit voltage, R_q internal resistance of the power source, U_S welding voltage, U_V sum of the voltage drops in the welding cable, I_S welding current, R_{Dr}, electrode resistance, R_{KD} transition resistance between contact-tube and wire. Here is

$$U_V = I_S \cdot (R_{WI} + R_{WA} + R_{Sp}) \qquad (3)$$

R_{WI} resistance of the workpiece lead, R_{WA} resistance of the connection of the workpiece, R_{Sp} resistance of the hose line. Usually, the displayed voltage U_m of the voltmeter integrated in the welding power source (voltage between the outputs of the power source) is called welding voltage. The real welding voltage U_S is between contact-tube and workpiece. The displayed voltage U_m is higher than the average welding voltage. The difference between the measured voltage and the average welding voltage is equal to the average sum of the voltage drops. Using an exact definition of the tapping point of the voltage either between torch and workpiece (Mp=O) or at the power source (Mp=l), the term "welding voltage" is clear.

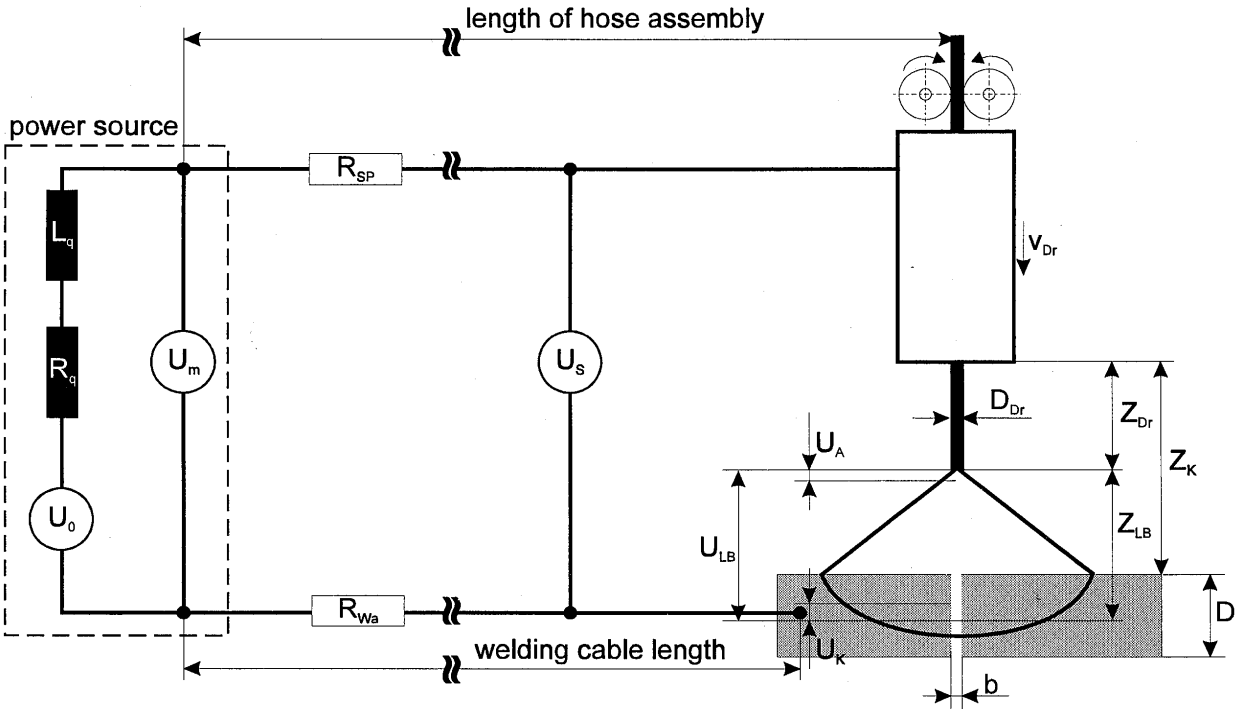

Figure1 : Process Scheme of the GMA-Weld Process (Equivalent Circuit)

$$U_S = U_m - M_P \cdot U_V \qquad (4)$$

At the surface of the wire end by absorption of electrons a power is created

$$P = I_S \cdot \left(U_A + \Phi + \frac{3}{2}\frac{kT}{e} \right) \qquad (5)$$

(Φ = work function of the electron in V, k = constant of Boltzmann, e = electrical elementary charge.) The joulean heat increases the enthalpy H_{Dr}, of the wire. The wire feed speed v_{Dr},, the welding current I_S, the enthalpy H_{Dr}, and the resistance of the wire e R_{Dr}, are connected as follows:

$$I_S = \frac{\rho \cdot v_{Dr} \cdot S \cdot (H_{Tr} - H_{Dr})}{U_A + \Phi + \frac{3}{2}\frac{kT}{e}} \cdot H_{Dr} = \frac{J_S \cdot I_S \cdot R_{Dr}}{\rho \cdot v_{Dr}}$$

$$R_{Dr} = \frac{1}{S}\int_o^{Z_{Dr}} \rho_{Dr}(H)\,dz \qquad (6)$$

(ρ = density of the workpiece material, S := wire cross section area, H_{Tr}, = enthalpy of the drop, H_{Dr}, = enthalpy of the wire extension, J_S= current density in the conductor, Z_{Dr}, = length of the wire extension, r_{Dr}, = specific resistance of the wire extension. These equations are valid only under the condition of a constant arc length Z_{Lb}.

$$Z_{Lb} = \frac{U_O - I_S \cdot R_q - U_V - U_A - U_K - I_S \cdot (R_{Dr} + R_{KD})}{E} \qquad (7)$$

If the length of the arc is changing, the wire extension (respectively the resistance of the wire electrode), the enthalpy of the wire extension and the welding current have to be corrected. The non-linear, implied given problem

$$I_S = f_1(v_{Dr},\ H_{Dr}) \qquad (8)$$

is only solvable iteratively. Therefore the temperature as a function of the enthalpy is complex:

$$H(T) = \int_o^T c_\rho(T)\,dT + \Psi(T) \cdot H_L$$

$$H_{Dr} = f_2(I_S, v_{Dr}, R_{Dr}) \quad R_{Dr} = f_3(v_{Dr}, H_{Dr}) \tag{9}$$

($0 \le \psi \le 1$ relative part of the liquid in the two phases zone, c_r = specific heat capacity at constant pressure, H_L = enthalpy of the weld pool, T = temperature). At the connection of the specific wire resistance and the enthalpy, the enthalpy H_C at Curie temperature has to be considered. For both differing cases the found connections are linear:

$$\rho_{Dr}(H) = \begin{cases} 25 + 0{,}164 \cdot H & bei H < H_C \\ 112 + 0{,}055 \cdot (H - H_C) & bei H > H_C \end{cases} [\mu\Omega \cdot cm] \tag{10}$$

with H = numerical value of H in [J/g]. The dependence of the cathode voltage drop, the voltage gradient in the arc column and the anode voltage drop on the welding current was approximated for the shielding gases argon and carbon dioxide by regression polynoms with the aid of empirical data[15, 16]. All dependencies on the percentage of the carbon dioxide r_{CO2} are described for various gas mixtures in following equation:

$$E(A_r + CO_2) = E(A_r) + \left[E(CO_2) - E(A_r)\right] \cdot \exp\left(\frac{-r_{CO_2}}{0{,}2}\right) \tag{11}$$

The drop temperature or drop enthalpy in argon is higher than in carbon dioxide and reaches its maximum in the combination of 82% argon and 18% carbon dioxide[17]. In practical application, the arc length during GMA-welding is not constant. This is why for UI-diagrams realistic values from 0.75 up to the double of the wire diameter are assumed. A comparison of the numerically derived weld voltage values with those achieved from test welds showed that for the description of the UI-diagrams (with slightly curved shape) mainly in the lower voltage range some additional factors have to be attended to. The average voltage, measured by customary moving-coil or digital instrument, is in the short-arc range approximately about 10-15% lower than the effective value. In the spray-arc range both values are about equal[16, 18].

The exception in the case of the short arc is due to the fact that, during the short-circuit duration the voltage practically equals zero while the current intensity is relatively high. The short circuit duration t_K diminishes the voltage efficiency by the factor:

$$\left(1 - \frac{t_k}{t_k + t_{Lb}}\right) \tag{12}$$

(t_{Lb} = arc duration). At the same time, the mean current intensity in short-arc welding I_{KLB} increases under consideration of the resistance R and the inductivity L in the total circuit by the factor:

$$\left(t_k \cdot \frac{R}{2 \cdot L}\right) \tag{13}$$

From that results:

$$I_{KLB} = I_S\left(1 + \frac{t_K}{t_K + t_{Lb}} \cdot \frac{t_K \cdot R}{2 \cdot L}\right) \tag{14}$$

For 0.05 Ω resistance, 0,4 mH inductivity, 4 ms short circuit duration and 20 ms arc duration, I_S increases by the factor 1.05 ($CI_{KLB} = 1.05\ I_S$). By means of a statistical analysis the dependence of the short-circuit frequency from the voltage can be determined. For the mixed gas (80% argon and 20% carbon dioxide) this dependence has been determined[19] and has been adopted for the calculation of the presented model. In spray-arc welding the short circuit duration is t_K = O. So, mean and effective values are about identical.

Figures 2 and **3** show that the slightly curved shape of the UI-diagram in the lower current range can be reproduced by means of the above-described factors.

2.2 Description of the Arc

For describing the arc, a model has been developed Tula University, Russia, **Fig. 4**. The conical arc model is able to reproduce the real situation rather good. The longer the arc length Z_{Lb}, the larger the arc radius R_{LB}. The radius R_{LB} results from:

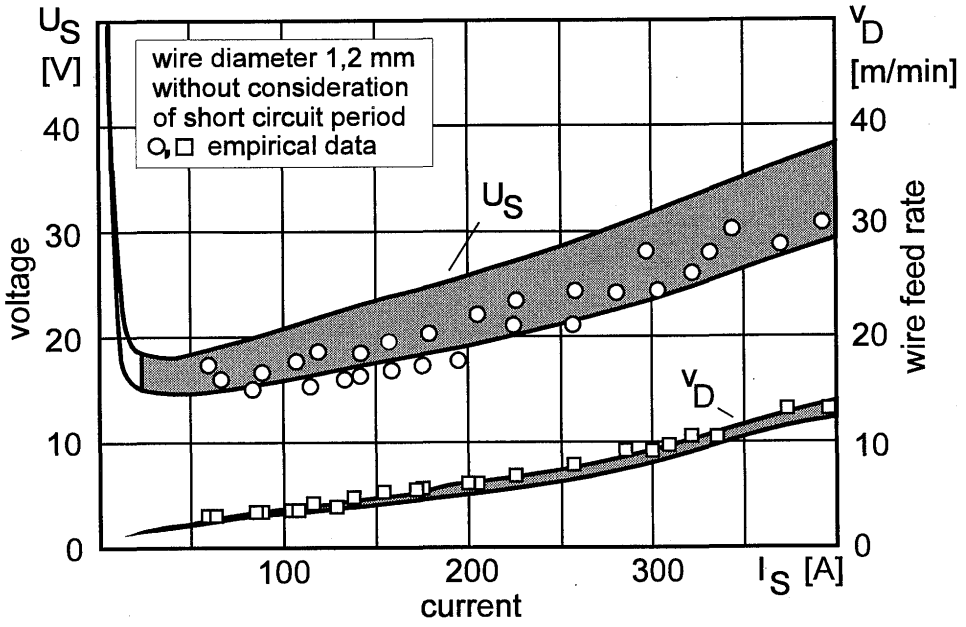

Figure2 : UI-Diagram without Consideration of the Short-Circuit Phase.

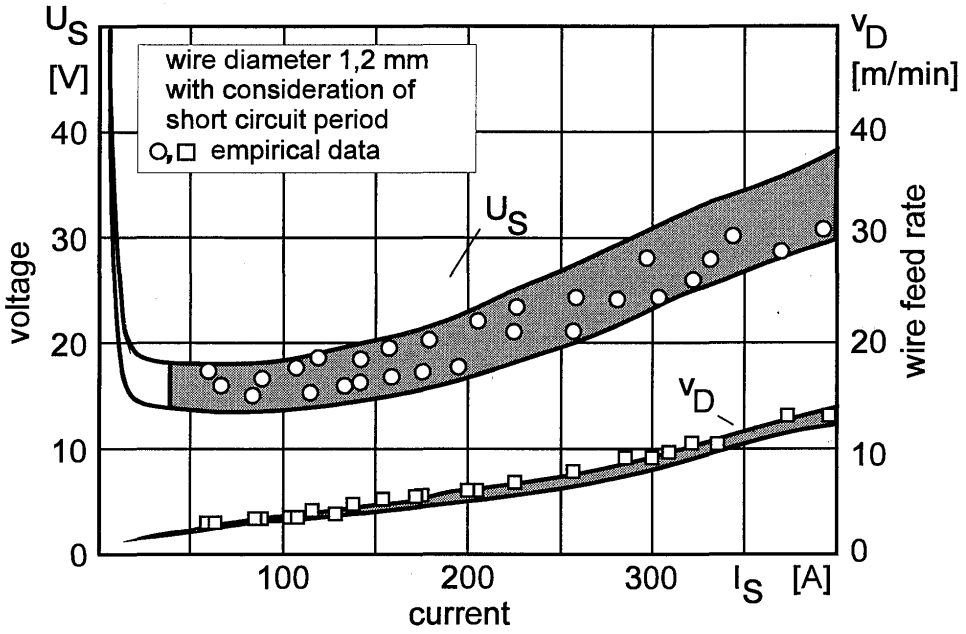

Figure3 : UI-Diagram with Consideration of the Short-Circuit Phase.

$$R_{LB} = \frac{D_{Dr}}{2} + Z_{Lb} \cdot \tan(\Theta) \qquad (15)$$

From the results of tests series, relations between the following angle sizes and the drop radius have been established:

$$\Theta_{CO_2} = 3,01 - 3,24 \cdot Z_{Lb}^{0,13} \cdot I_S^{-0,074}$$
$$\Theta_{82/18} = 1,79 - 7,11 \cdot Z_{Lb}^{0,6} \cdot I_S^{-0,31} \qquad (16)$$
$$R_{Tr} = \begin{cases} 1,25 \cdot R_{Lb}\,(KLB) \\ 0,7 \cdot R_{Lb}\,(SLB) \end{cases}$$

where the values for Z_{Lb} have to be introduced in cm, I_S in Ampere and where Θ is defined by circular measure.

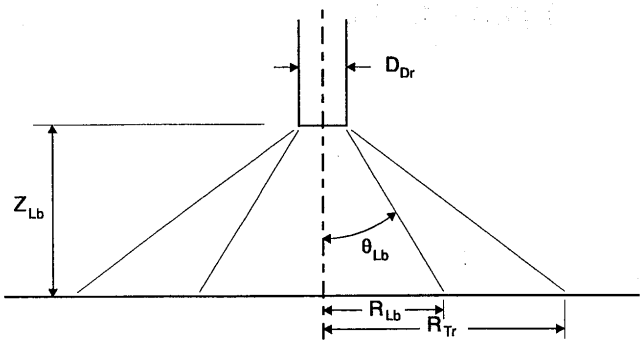

Figure4 : Arc Model and Definition of the Characteristic Values (D_{Dr} wire diameter, Z_{Lb} arc lenght, Θ_{Lb} angle of the arc cone, R_{Lb} arc radius, R_{Tr} drop radius)

2.3 Thermal Processes in the Weld Workpieces

The thermodynamical condition of the workpiece is described during the welding process in a 3D-system of coordinates by means of the energy conservation equation[7]:

$$\rho\frac{\partial H}{\partial t}+v_S\rho\frac{\partial H}{\partial x}+\vec{\nabla}\cdot\left(\rho H\vec{v}_k\right)=\vec{\nabla}\cdot\left(\lambda\vec{\nabla}T\right) \qquad (17)$$

(v_S = Welding Speed, v_k= weld pool convection speed, λ = thermal conductivity). For the heat flow in GMA-welding which stands as a boundary condition for the solution, the arc power P_{Lb} as well as the drop performance P_{Tr}, are considered. One part of the power P_{Lb} takes effect on the workpiece surface (P_{Ob}), the other part dissipates through the gap (P_{Sp}). The powers are considered as normally distributed.

$$P_{Sp}=P_{Lb}\frac{2\cdot b}{\pi\cdot r_1} \qquad P_{Ob}=P_{Lb}-P_{Sp} \qquad (18)$$

(r_t = outer radius of the thermal normal source, b = gap width). On the workpiece surface the following boundary conditions for the geometric distribution of the input power P_{Ob} and P_{Tr}, as well as for the heat exchange by convection, radiation and evaporation have to be fulfilled:

$$-\lambda\frac{\partial T}{\partial z}=\frac{3\cdot\eta_{Ob}\cdot P_{Ob}}{\pi\cdot r_{Ob}^2}\cdot\exp\left(-3\cdot\frac{r^2}{r_{Ob}^2}\right)$$
$$+\frac{3\cdot\eta_{Tr}\cdot P_{Tr}}{\pi\cdot r_{Tr}^2}\cdot\exp\left(-3\cdot\frac{r^2}{r_{Tr}^2}\right) \qquad (19)$$
$$-\alpha_0(T)\cdot\left(T-T_0\right)-q_v\cdot\exp\left(-\frac{H_v}{RT}\right)$$

(r = radial distance of the heat source centre, λ = heat conductivity, η_{Ob} = efficiency of the thermal energy input over the workpiece surface, η_{Tr} = efficiency of the drop heat, r_{Ob} = measure for the power distribution spectrum on the surface, r_{Tr} = measure for the drop performance distribution, α_0= combined heat transfer coefficient for convection and radiation, q_V = heat flow density of the evaporation, R universal gas constant, H_V = evaporation enthalpy, T_0 = ambient temperature).

For the surface, the "power distribution" has been established as follows:

$$-\lambda\frac{\partial T}{\partial z}=\frac{\eta_{Ob}\cdot P_{Ob}}{r_{Ob}\cdot d}\cdot\exp\left(-3\cdot\frac{r^2}{r_l^2}\right) \qquad (20)$$

(d = sheet thickness). For the work piece bottom side the following boundary conditions are applicable:

$$-\lambda\frac{\partial T}{\partial z}=A_0\left(T-T_0\right) \qquad (21)$$

where A_0 is defined as the heat transfer coefficient that considers heat transfer from the workpiece into the probably used backing (e.g. copper bar).

2.4 Hydrodynamical Processes in the Molten Pool

The coordinates Z_o (= $Z_o(x,y)$ Z-coordinate of the upper molten pool surface) and Z_u ($Z_u(x,y)$ Z-coordinate of the lower molten pool surface) for the weld pool, **Fig. 5**, are results from the differential equation[7]:

$$\sigma(T)\vec{\nabla}\cdot\frac{Z_o'}{\sqrt{1+\left(Z_o'\right)^2}}-\rho g Z_o$$
$$=\Gamma+\frac{P_{Lb}\cdot\exp\left(-3\frac{r^2}{r_l^2}\right)}{\sqrt{1+\left(Z_o'\right)^2}}+P_D(T) \qquad (22)$$

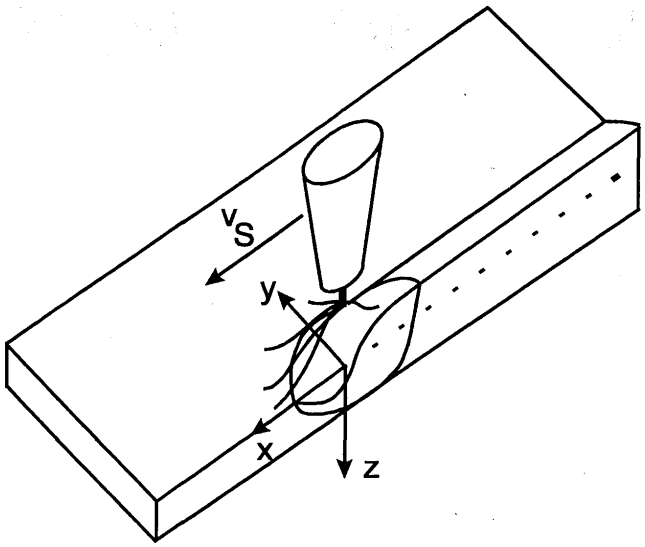

Figure5 : Definition of the used Coordinate System.

$$\sigma(T)\vec{\nabla}\cdot\frac{Z_u'}{\sqrt{1+(Z_u')^2}}-\rho g Z_u=\Gamma \qquad (23)$$

where P_{LB} = the maximum arc pressure, P_D = vapour pressure, Z'_o = two dimensional divergence of Z_o, Z'_u = two dimensional divergence of Z_u, ρ = mass density of the molten metal, g = gravitational constant, T = temperature inside the workpiece. The constant Γ has to be chosen thus that during the liquid phase, the condition for keeping the mass balance is a given quantity:

$$2\cdot\int_o^n (Z_o+Z_u)dy = d\cdot(b-B)+\frac{\pi\cdot D_{Dr}^2\cdot v_{Dr}}{4\cdot v_s} \qquad (24)$$

(n = y-coordinate of the weld boundary, d = sheet thickness, b = gap width, B = transverse shrinkage of the weld parts , D_{Dr}, = wire diameter). The following boundary conditions for the fusion area (a) and the crystallisation front (b) have to be attended to:

$$(a)Z_o=\begin{cases}0 & for Z_o<Z_t\\ Z_t & for Z_o>Z_t\end{cases}\quad (b)\frac{dZ_o}{dx}=0 \qquad (25)$$

Here $Z_t = Z_t(x,y)$ stands for the fixed weld pool profile. When welding thin sheets the following boundary conditions are also to be taken into consideration.

$$(a)Z_u=-d\quad (b)\frac{dZ_u}{dx}=0 \qquad (26)$$

2.5 Calculation

The equation (17) is calculated by means of the four Navier-Stokes-equations. The equation is not very complicated, the numerical solution, however, can be achieved only by means of a large computer system and needs a great deal of time. For the consideration of the weld pool convection in the overall model, the numerical calculation would take more than two hours on a large computer just to perform the two-dimensional calculation task[20]. In spite of that proof could be furnished[7] that a good prediction of the weld shape, for example, and of undercuts is possible when reasonable simplifications are used, also when applying the otherwise unchanged algorithms.

In most practice-oriented cases h is sufficient to just calculate a quasi-stationary weld formation. When welding thin sheets the convective heat flow value is negligible. This simplification can be compensated in good approximation by increasing the heat conduction by the factor:

$$\varepsilon_k=\left(2-\frac{T_l}{T}\right) \qquad (27)$$

(T = temperature inside the workpiece, T_l = liquidus temperature)[7]. In that case (17) is simplified to:

$$v_s c_p \rho\frac{\partial T}{\partial x}=\vec{\nabla}\cdot\left(\varepsilon_k\lambda\vec{\nabla}T\right) \qquad (28)$$

with the above-mentioned boundary conditions. The equation system can be numerically solved by the Finite Element Method with most simple explicit differential methods. In this case, the convergence condition (with small step sizes in the grid system) has to be strictly adhered to. For this reason, the system was solved by the implicit differential method, which is convergent towards optional intervals. The flow chart, as a computation rule for the equation system, was established after the economical "Local-1-D-method" (by means of the analysis

of multidimensional tasks in sequence of one-dimensional tasks, economical additive differential methods for differential equations in complicated fields can be established). A personal computer (486) with a repetition rate of 66 MHz takes just a few seconds for the model computation and that despite the non-linear connections between weld voltage, weld current and arc length as well as the consideration of the thermo-physical material data.

3. Analysis System for GMA-Welding of Thin Steel Plates

Welding quality assurance in automated arc welding increasingly demands for the optimisation of the weld process. Without information about the weld size, however, empirical or arithmetical optimisation of the weld quality is impossible. The deterministic model for GMA-welding, as described above[22] allows to solve optimisation tasks in regard of several criteria. A numerical 3D-model that describes the physical fundamentals of GMA-welding enables detailed process investigations. Based on this level the task is to achieve a solution of the so-called "inversal task", "Inversal task" means the determination of weld parameters in dependence of the weld sizes. Three arithmetical conditions which have to be fulfilled for solving this task can be formularised: The solution has to be existent, it has to be unique and also to be stable.

There is no unique solution for welding processes as a certain weld shape can be achieved by various parameter combinations. In order to select one solution from this variety it is necessary to formularise a secondary condition. This can be done, for example, by a maximisation condition. The demand for stability causes a steady dependency of the output data on the input data. It is most important to attend to this condition during process simulation of that particular range of parameters where unsufficient through-welding or burn- through occur.

3.1 Formulisation of the Task

For the initial task which was the determination of the weld sizes in dependence of the weld parameters, the following definitions apply:

$$X=(x_1, x_2, \ldots, x_n)$$
$$Y=(y_1, y_2, \ldots, y_n)$$
$$Y=f(X)$$

where x_i stands for the input data and y_i for the output data. This enables a description of the dependency of the output data on the input data by the vector valent function f. The input data can be subdivided into two categories. Welding current I_S, welding voltage U_S and welding speed v_S belong to the variable input data. The material (thermophysical properties), sheet thickness, gap width, wire diameter D_{Dr}, contact-tube distance Z_K and shielding gas S_G (thermal and electrical conductivity, voltage gradient of the arc column) belong to the fixed input data. The output data are the weld parameters according to DIN EN 25817[23]. In this case, top reinforcement (h_N) and root reinforcement (h_W), weld width (b_N) and root width (b_W) as well as existence and size of undercuts (n_K) are regarded.

In technological production preparing the parameters I_S, U_S, v_S have by means of the optimisation method to be selected thus that the weld geometry fulfills certain requirements (e.g. after DIN EN 25817) and, likewise, the optimum value of a previously defined objective function (e.g. weld defects, productivity) is achieved. As an example the solution of the inversal task in GMA-welding of thin unalloyed steel plates is regarded. The objective is to achieve the values for I_S, U_S and v_S under consideration of the objective function F. The possible range of solutions is characterised by the following restrictions:

$$I_{min} < I_S < I_{max} \quad (29)$$
$$U_S=f(I_S, D_{Dr}, Z_K, S_G) \quad (30)$$
$$v_S > 0 \quad (31)$$

Moreover, the following conditions have to be fulfilled in order to find a solution:

$$b_W > \varepsilon_W \text{(full penetration)} \quad (32)$$
$$Z_W'' > \varepsilon_Z \text{(no burn-through)} \quad (33)$$
$$F=F_{opt} \text{(objective function is optimally fulfilled)} \quad (34)$$

Here, b_W stands for the weld width on the sheet bottom side and Z_W"or the second derivation of the function that describes the weld under surface[22]. The values I_{min} and I_{max} are calculated from the UI-diagram $U_S = f(I_S, D_{Dr}, Z_K, S_G)$ under consideration of contact-tube distance, wire diameter, shielding gas type as well as data of the transfer to other process regions, **Fig. 16**. ε_W and ε_Z are to be valued as "safety distance". Should the values of b_W and Z_W" be higher, the stability of the solutions will be guaranteed despite computing tolerances.

The case Z_W"=O stands for the mathematical limiting case where the weld bum-through first occurs. If a combination of the fixed parameters does not allow a solution under the above-mentioned conditions, the values contact-tube distance, gap width, shielding gas type and wire diameter have to be changed according to the defined sheet thickness.

4. Description of the Software MAGSIM for Simulation of Weld Formation

The above-mentioned theoretical expositions about establishing a model of the GMA-welding process led to the development of the simulation software MAGSIM for predicting the weld quality. The software has to fulfill the following tasks:

A) Calculation of the electric arc parameters depending on no-load voltage, electric resistances of power source and welding cable, shielding gas type, weld speed, wire feed speed, wire diameter, contact-tube distance and also the thermal energy in the workpiece, caused by pre-heating.

B) Calculation and analysis of weld shape as well as weld defects (incomplete fusion, exceeding of pre-determined measures for top and root reinforcements, penetration depth, burnthrough), according to DIN EN 25817 for the specified material as well as of the sheet thickness at specified weld parameters under consideration of the gap and a possible

C) Determination of optimum weld parameters to ensure the requested objectives (maximum product capacity or maximum certainty of weld quality under consideration of process parameter tolerances).

D) Process diagnosis for the solution of different questions that refer to the practice, e.g., how to assess parameter variation influences onto the weld dimensions.

4.1 MAGSIM-Program Design

The program consists of three modules for the analysis of results, process diagnosis and for process optimisation which shall be explained in detail. For calculating, 25 parameters are taken into account:

The fixed input data:

A) Task description
- 1) Steel — unalloyed steel; low-alloy steel; CrNi steel
- 2) Sheet thickness — 0,5 .....5,0mm
- 3) Evaluation groups — DIN EN 25817,

B) Description of the welding equipment
- 4) Power source slope — 0,0 - 5,0 V/100 A
- 5) Min. no-load voltage — 15,0 - 30,0 V
- 6) Max. no-load voltage — 20,0 - 50,0 V
- 7) Length of hose assembly — 0,5 - 10,0m
- 8) Length of workpiece cable — 0,5 - 10,0m
- 9) Location of voltage measuring — torch/power source
- 10) Shielding gases — C02; 82%Ar 18%C02; 92%Ar 8%C0
- 11) Wire diameter — 0,8/1,0/1,2/1,4mm
- 12) Contact-tube distance — 5,0 - 25,0 mm

C) Technological conditions
- 13) Gap width — 0,0 - 4, 0mm
- 14) Backing — Yes/No
- 15) Groove — Yes/No
- 16) Groove shape — rounded/square
- 17) Groove width — 0,0 - 10,0 mm
- 18) Groove depth — 0,0 - 3,0 mm
- 19) Workpiece temperature — O - 300℃

The variable input data:
- 20) Welding current — 50-360A
- 21) Welding voltage — 13-40V
- 22) Welding speed — 25-240 cm/min
- 23) Current tolerance range — 0,0 - 6,0 %
- 24) Voltage tolerance range — 0,0 - 6,0 %
- 25) Weld speed tolerance range — 0,0-6,0 %

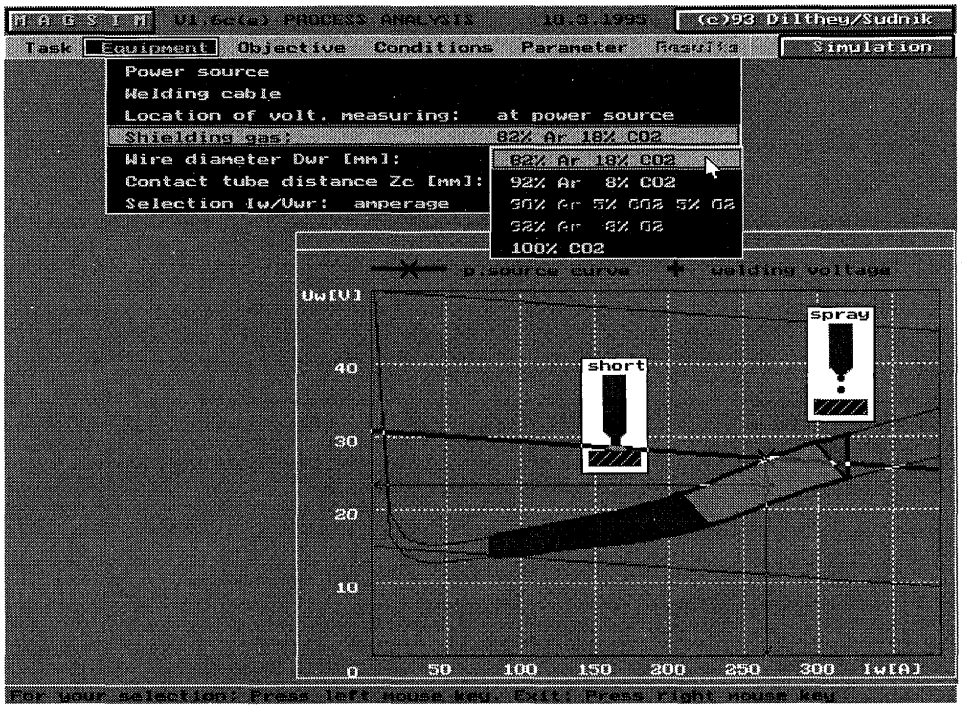

Figure6 : The UI-Diagram.

4.2 The Software Module "UI-Diagram"

Fig. 6.

During the input or the alteration of parameter values for weld current and voltage, the respective operating point is, by means of the software module "UI-diagram" subject to a running update shown as a UI-diagram on the monitor. Here, the admissible process limits in accordance to instruction sheet DVS 0926, for the short-arc as well as the spray-arc and the long-arc are marked as coloured zones, **Fig. 6**.

Here, as an option, the operating point can be defined over the input of weld current Is or wire speed rate v_D. The electric (current, voltage) and the energetic (energy efficiency ratios of arc heat flow and droplet heat flow) parameters are specified by the potential-, mass- and energy balance at the weld contour. The module algorithms describe the electric and energetic characteristics of the weld task. The thus achieved data are necessary for the solution of the heat condition equations.

4.3 The Software Module "Analysis"

The data acquired by the "UI-diagram" module are used by the software module "Analysis" in order to calculate the thermo-physical processes at the square butt joint. The capacity of the software-module "Analysis" is best described as follows see also **Fig. 7**:

- Analysis of the weld formation and numerical calculation of:
  -3D-fields of temperature, assisted by the finite differences technique (FDT)
  - thermal cycles of the weld pool centre at the sheet top and bottom side
  - 3D-profile of the weld pool and 2D weld shape by means of the FDT
- Geometrical data of the weld seam and the HAZ-contour
- Automatic evaluation of the weldquality according to DIN EN 25 817.

The computer simulation enables the user to easily investigate how parameter variations effect a possible weld result, **Fig. 8 a - c.** The calculated results were subject to investigations by comparative weld tests and by literature data and they showed throughout good up to very good conformity in the weld formation. The input of data shift values for the determination of "GMA-weld data for square butt welds",

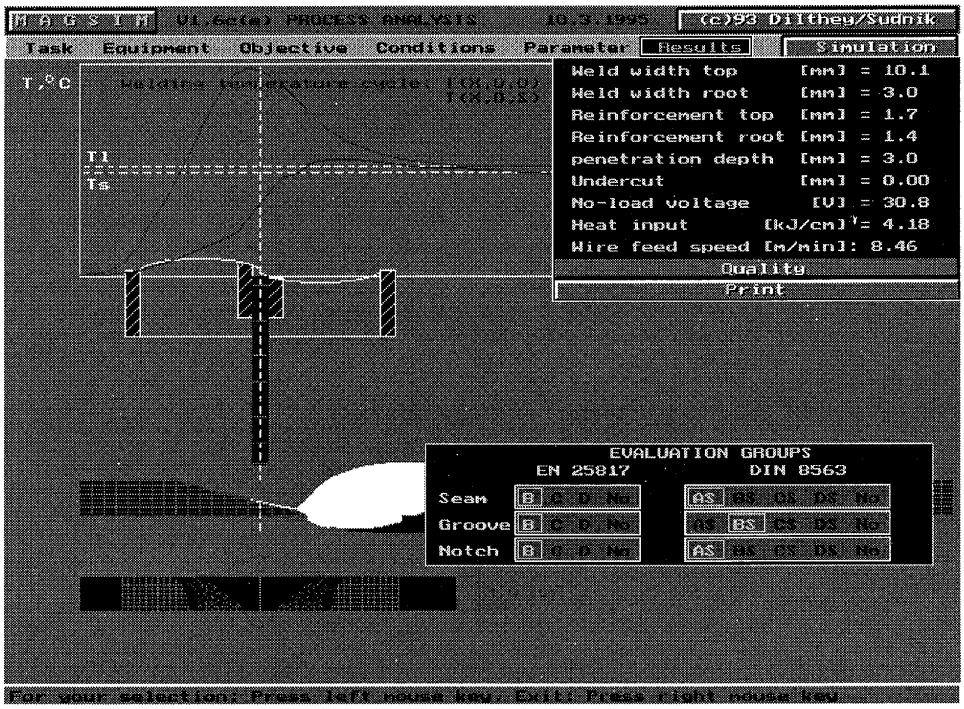

Figure7 : Calculation of Weld Pool and Seam Profile with Evaluation according to DIN EN25817welding parameter : shielding gas 82%Ar+18%CO_2, sheet thickness 3mm, gap width b=0mm, welding current Is=295A, voltage Us =27V, welding speed Vs=89cm/min, wire diameter D_{Dr}=1, 2mm, contact-tube-distance Z_K=14mm

carried out by a well-known welding company, gave a generally good evaluation of the weld results according to DIN EN 25 817.

4.4 The Software Module "Optimisation"

Recently developed algorithms as well as a numerical 3D-model of the GMA-weld process are the basis for the optimisation of GMA-weld process parameters. The optimisation criteria can be chosen from among maximum productivity, e.g., or maximum achievable good quality certainty, even if parameter variations are prevalent. In technological production planing, the parameters weld current I_S, weld voltage U_S as well as weld speed v_S have, by means of a suited optimisation method to be selected thus that the weld geometry can meet certain demands (e.g. DIN EN 25 817) and, likewise, fulfill the optimum value of a previously defined objective function (e.g. the number of weld defects, weld time).

The fixed input data are: material (its thermo-physical properties), sheet thickness, gap width, wire diameter, contact-tube distance, and shielding gas type (voltage gradient in the arc column). Variable input data are the weld parameters I_S, U_S and v_S. The output data are top and root reinforcements (h_N and h_W) or weld width and root width (b_N and b_W) and undercuts (h_K). To solve the tasks, the proceedings should be as follows:

1. Arrangement of the 3D-system of coordinates in order to picture the operating point A (I_S, U_S, v_S) and its listing into the UI-diagram

2. Determination of the maximum permissible current in dependence on the wire diameter

3. Calculation of the weld voltage $U_{so} = f(I_{so})$

4. Determination of the maximum possible welding speed v_{max}, where the root width equals Zero (insufficient fusion)

5. Determination of the minimum weld speed v_{min} where burn-through occurs

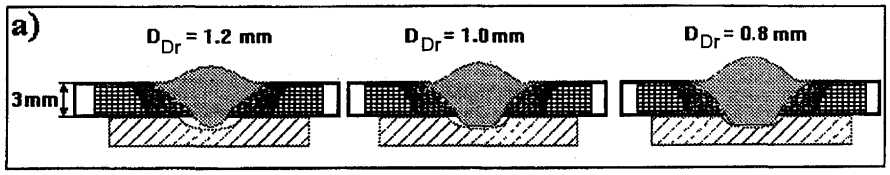

I_S = 250 A; U_S = 24 V; v_S = 72 cm/min; Z_K = 14 mm

shielding gas: 82%Ar + 18% CO_2

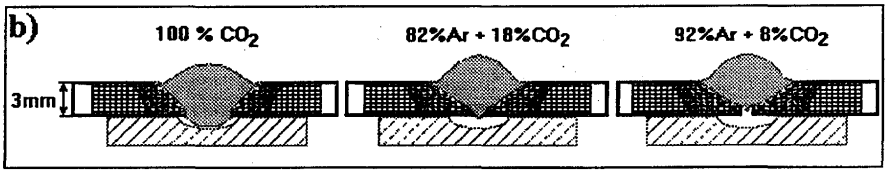

D_{dr} = 1,2 mm; I_S = 195 A; U_S = 22 V; v_S = 50 cm/min; Z_K = 14 mm

(short arc welding)

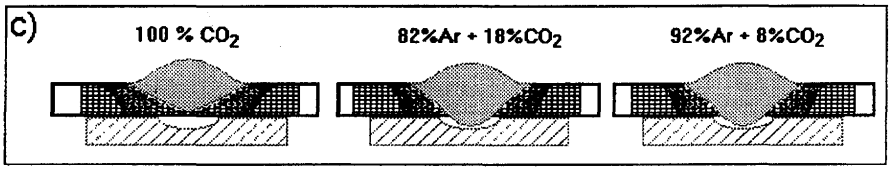

D_{dr} = 1,0 mm; I_S = 250 A; U_S = 25 V; v_S = 70 cm/min; Z_K = 12 mm

(spray arc welding)

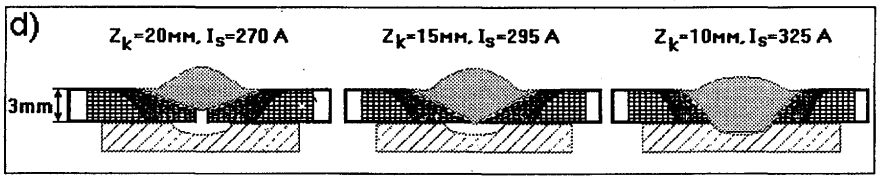

v_{Dr} = 8,8 m/min; U_S = 29 V; v_S = 100 cm/min; D_{dr} = 1,0 mm

shielding gas: 82%Ar + 18% CO_2

Figure8 : Material : unalloyed steel, sheet thickness 3mm, gap width b=1mm, a) Results with variation of the parameter "wire diameter (D_{Dr})" b) Results with variation of the parameter "shielding gas" (short arc welding) c) Results with variation of the parameter "shielding gas" (spray arc welding) d) Results with variation of the parameter "contact-tube-distance (Z_k)"

6. Calculation of the optimum weld speed, including the "maximum security interval" $v_{so} = (V_{min} + V_{max})/2$.

7. Calculation of the variation coefficient P_i = $0,5\ (V_{max} - V_{min})/vs$.

8. Iteration for next current and calculation of the variation coefficient

9. Selection of the maximum P_i as the optimum value and storing of the appropriate optimum parameters I_{so}, v_{so} and U_{so}

The monitor displaying the results of a process optimisation is depicted in **Fig. 9.**

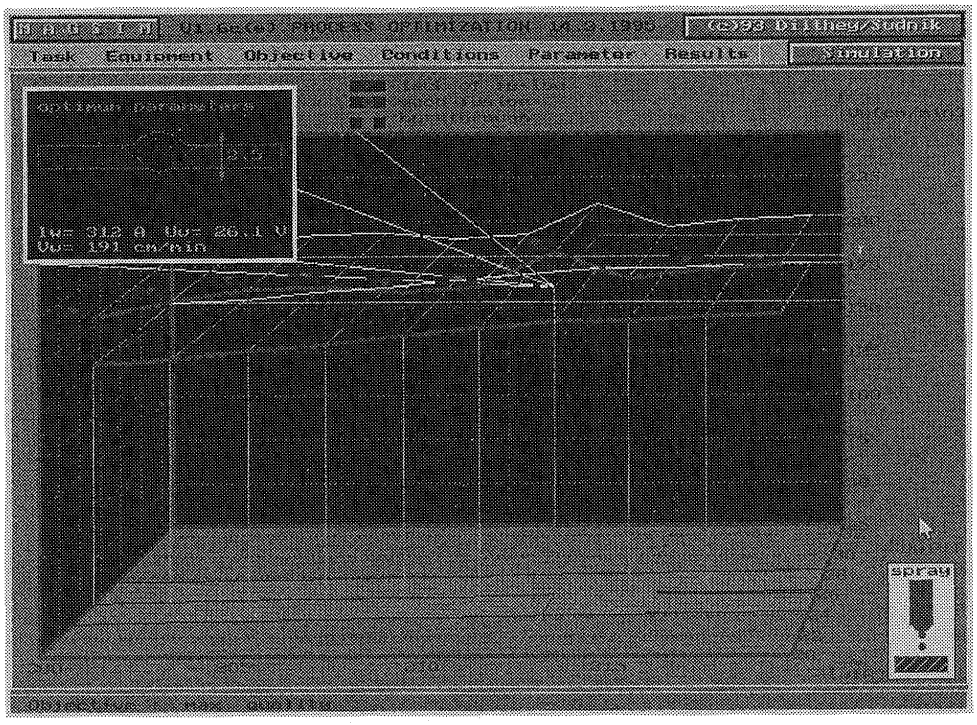

Figure9 : Result of a Process Optimisation within the Allowable Working Range.

4.5 The Software Module "Diagnosis"

Further findings can be derived from statistical analyses when parameters depending on tolerances are prevalent. For that, the software module "Diagnosis" has been developed. The solution of different practical optimisation tasks entails the problem of considering parameter variations. Substantial information about scattering of the weld geometry can be derived from the statistical analysis and/or the Monte-Carlo technique. The characteristics for the statistical distribution of the process parameters (current, voltage, weld speed, etc.) around the operating point serve as input data for the statistical analysis. The calculated result includes the statistical characteristics of the distribution and the weld geometries resulting from it.

The generating of stochastic values for the tolerance-dependent parameters is done by means of an algorithm that is based on the method of an inverted function as well as the splineinterpolation. Therefore, a function for the generating of a standardised Gossip distribution for the variable x with a mean value m_x and the standard deviation s_x is applied. For the expected value m_x of the influence variables, the nominal values of the weld current, the weld voltage, the weld speed, and, for the standard deviation, a third of the permissible deviation, are used.

While the 3D-simulation of the GMA-welding process takes only approx. a few seconds of computing time on a PC 486 (66 MHz), sampling by means of the Monte-Carlo technique takes substantially more time, even on a computer that works considerably faster. A possible way, therefore, is the conversion of the 3D-micro-model by means of numerical convolution into the polynomial form of the macro-model. From a factor plan with 8 diagonally positioned corners of the investigated tolerance zone and from the centre point by means of the here presented simulation at the 3D-micro-model the appropriate weld results are determined. In order to achieve the linear relation between the geometrical characteristics of weld and process parameters, the results of the 3D-micro-model are used for the establishing of a valid(within the limits of the tolerance zone) macro-model by creating a polynomial relation between input- and output data

$$y_j = a_{oj} + a_{1j}x_1 + a_{2j}x_2 + a_{3j}x_3$$

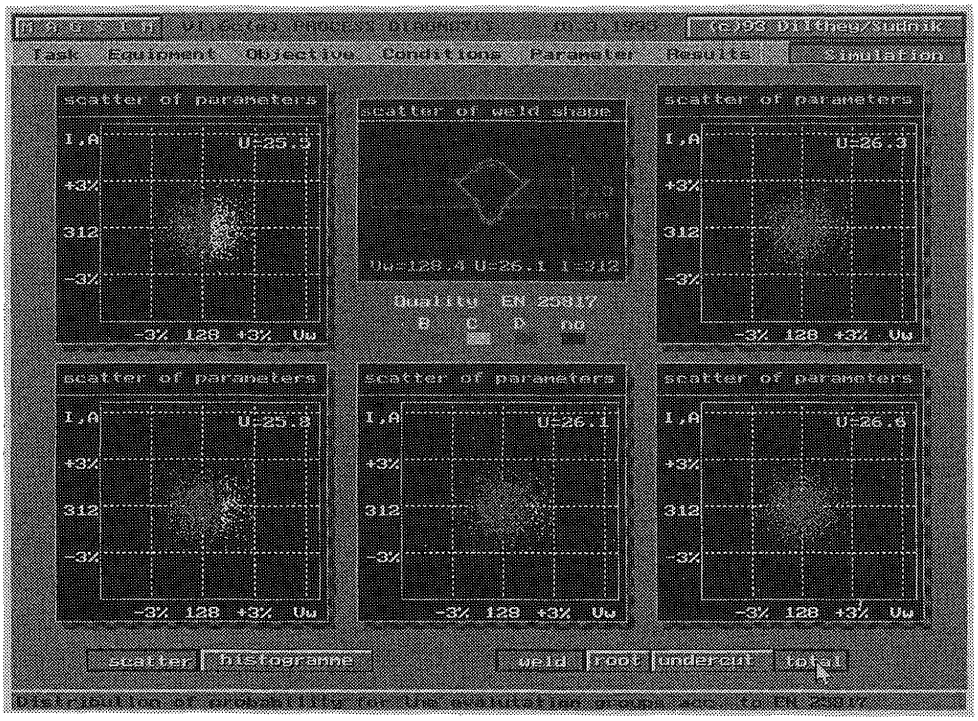

Figure10 : Probability Distribution of Evaluation Groups According to DIN EN25817

This formula shows the dependence between weld size y_j and the process parameters x_j' in correspondence to I_S, U_S and v_s. The determined 5 equations for the 5 weld parameters seam-and root-width, top-and root-reinforcement as well as undercut depth, therefore stand for the reduced models of the analysed process in the zone of parameter tolerances around the chosen operating point. Subsequently, process simulation is done by means of the polynomial 5 macro-model equations, derived from the 9 simulations. The parameters of the five macro-model equations are stochastic values within the zones of $I_S \pm \Delta I_S$, $v_S \pm \Delta v_S$ and $U_S \pm \Delta U_S$.

For the statistical probability evaluation by means of the Monte-Carlo technique, a sufficiently high number of simulation runs is carried out. This is possible, because of the specified macro-model equations, in short time on a customary PC. The associated probability is specified over the relative frequency of the results in a certain evaluation group. The results of the statistical evaluation are displayed in three histograms for seam, root and undercuts, which show the frequency of the association with a certain evaluation group. It is also possible to entirely evaluate the weld quality by means of checking the parallel associations to an evaluation group, **Fig. 7**. Another way of demonstrating the weld quality is the scatter diagram of the weld parameters, where the evaluation group with scaling of the hitting frequency in a group is identified by different colors, **Fig.10.**

At pre-defined nominal values as well as at tolerances of weld current and weld speed a preferential direction can be noticed, where the nominal point of the parameter vector should be shifted at. As a quasi-3D-monitor representation has not proved successful, the graphical display was designed so that at a voltage U_S fixed in 5 intervals, the scatter fields for seam, root and undercuts and a complete evaluation can be calculated and displayed. The necessary 2000 Monte-Carlo runs at the macro-model use just a few seconds of computer time.

5. Comparison of the Calculated Results and Test Results in GMA-Welding

For this comparison, empirical data from literature have been adopted and tests were carried out. Best accordance was achieved from

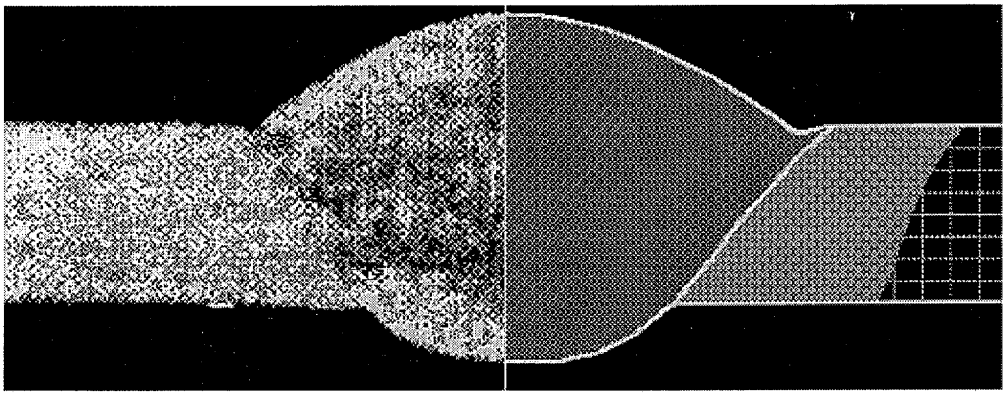

Figure11 : Comparison of the Weld Formation achieved from Test Welds (left) and achieved by Calculation with the MAGSIM Program (right) welding parameters : shielding gas 82%Ar+18%CO_2, welding current Is=260A, welding voltage Us=24, 5V, welding speed Vs=60cm/min, wire diameter D_{Dr}=1, 2mm contact-tube-distance : Z_K=12mm

tests, made with sheet thickness of 3 to 5mm using the shielding gases carbon dioxide and 82% Ar + 18% $C0_2$[21]. **Figure 11** shows the comparison between the weld formation achieved from weld tests and the weld formation that has been calculated by the simulation program.

6. Further Development

The program is subject to steadily further development and also further enlargement by addition of other materials, varying wire diameters, shielding gases, groove geometries, process variations and welding positions.

6.1 Pulsed-Arc Welding

Within the scope of a research project a model of the pulsed arc heat source was developed. The new module for MAGSIM, based upon this efficient model, allows the prediction of pulsed GMA-welding processes and their weld results. An energetic analysis of the total welding circuit in consideration of the static (base and pulse phase) and dynamic(leading and trailing edge of pulse current) characteristics of the power source, the dynamics of electrode wire bum-off and the change of arc length was carried out. With it the effective power of the pulse heat source results from the product of the effective current $i_S(t)$ and voltage $u_S(t)$:

$$Q_{eff} = \frac{\eta_{eff}}{t_P + t_B} \int_0^{t_{IMP}} i_s(t) u_s(t) dt \qquad (35)$$

η_{eff} is the effective efficiency of the pulse arc determined by experimentally found data[24]. It depends on the actual welding parameters and amounts to about 80 .... 85%. The mean values of current and voltage result from:

$$I_M = \frac{1}{t_P + t_B} \int_0^{t_P + t_B} i_s(t) dt$$
$$\text{and} \quad U_M = \frac{1}{t_P + t_B} \int_0^{t_P + t_B} u_s(t) dt \qquad (36)$$

The effective current and voltage are defined by:

$$I_{eff} = \sqrt{\frac{1}{t_P + t_B} \int_0^{t_P + t_B} i_s^2(t) dt}$$
$$\text{and} \quad U_{eff} = \sqrt{\frac{1}{t_P + t_B} \int_0^{t_P + t_B} u_s^2(t) dt} \qquad (37)$$

The partial model of the non-short-circuiting material transfer takes the electro-magnetic forces, the forces resulting from the surface tension and the gravitational force into consideration. The nonlinear interaction among the parameters makes a numerical solution of the problem necessary. As a result of the computer simulation the current and voltage curve of the process and the UI-diagram for base and pulse phase are shown on the screen, **Fig. 12.**

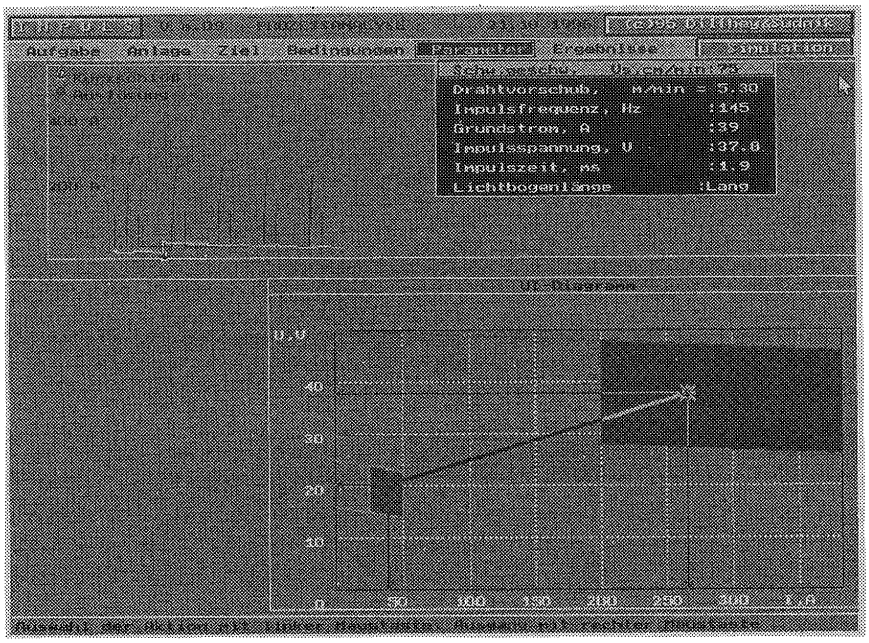

Figure12 : Results of the Numerically Calculated Pulsed-Arc Welding Process with UI-Diagram for Base-Phase and Pulse-Phase.

6.2 Fillet Welds

First results of the analysis module for fillet welds, which is still under development, are shown in **Fig.13**.

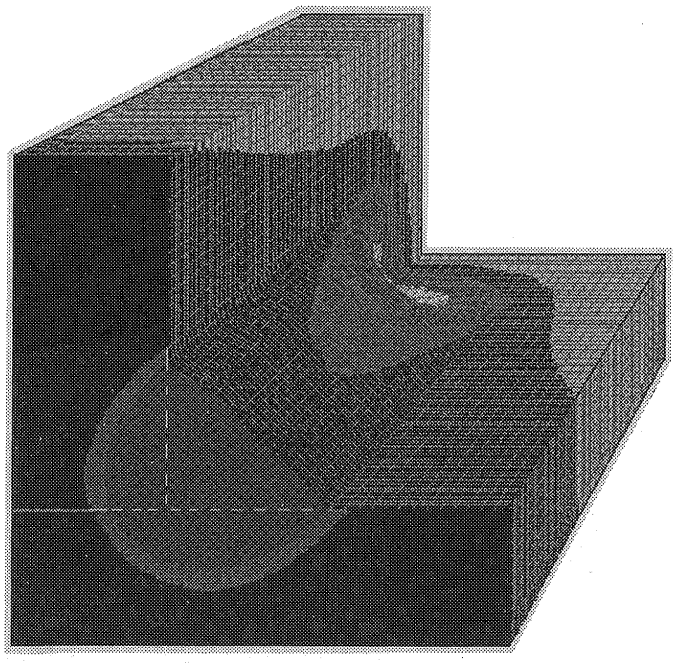

Figure13 : 3D-Display of a Simulated Fillet Weld.

7. Conclusions

The numerical description of the GMA-welding process and the simulation software resulting from it shall, on the one hand, be a means for the user in the prediction of weld formation under consideration of all relevant parameters and, on the other hand, are these investigations of assistance in completing quantitative knowledge about the physics in welding processes.

During many years of cooperation between the ISF Welding Institute of Aachen University, Germany, and Tula University, Russia, the simulation software MAGSIM has been developed and put into a commercially available release. It was published in several languages. The simulation software is fitted as tools for the training in welding technology and for the production scheduling of GMA-welding processes.

References

1) Baum, L., u. V. Fichter: Der Schutzgas-Schweißer.DVS-Verlag, Düsseldorf1990.
2) Timtschenko,W.A.u.a.:Programmierung von Schweißparametern für das MAG- Schweißene mit Robotern. Autom. Weld., Kiew (1989), H.1,S.44/47.

3) Dubuweckji, S.D u. O. G. Kasatkin: Optimierung der Schweißparameter anhand von Regressionsmodellen zur Nahtausbildung (russisch). Mathematische Methoden für das Schweißen, S.102/11, Paton Institut, Kiew 1986
4) Matthes K. J.,u.W.Renatus:Automatisierung des MAG-Schweißens von Stumpfnähten. Schweißtechnik 36 (1986), H. 12, S. 536/38.
5) Ohij, T., u. K. Nishiguchi: Mathematical modelling of a molten poof in arcwelding of thin plate: Technology Report of the Osaka Univ. 33 (1983), H. 1688, S. 35/43
6) Na, S. J., u. J Ruge: Temperaturfelder beim Schweißen von, Aluminiumdruckguß Schw. Schn. 42(1990), H. 7, S. 327/32.
7) Sudnik, W. A.: Untersuchung von Schmelzschweißtechnologien anhand physikalisch-mathematischer Modelle. Schw. Sch 43 (1991), H. 10, S. 588/90.
8) Engelst, W., u.a.: Mathematische Modellierung des elektrischen Lichtbogens (russisch), Verlag ILIM, Frunse 1983.
9) Tsao, K. u. S. Wu: Fluid Flow and Heat Transfer in GMA Weld. Welding Journal 67 (1988), H. 7, S. 150/56.
10) Ando, K., u. K. Nishiguchi: Mechanism of Formation fo Pencil-Point-Like Wire Tip in MIGArcWelding:Relation between the Temperature of molten Drop, Wire Extension and Heat Conductivity. IIW-Dok. 212-156- 68.
11) Ando, K., u. K. Nishiguchi: Average Temperature of the Molten Poof in TIG and MIG Arc Welding of Steel and Aiuminium. IIW-Dok. 212-161-68.
12) Tekrival, P., u. J. Mazumder: Finite Element Modelling of Arc Welding Processes. Welding Journal 67 (1988), H. 7, S. 150/56.
13) Pardo, E., u. D. Weckmann: Prediction of Weld Pool and Reinforcement Dimension of GMA Welds Using a Finite-Element-Model, Metallurgical Trans.20B (1988), H. 12, S. 937/47.
14) Allum, C. J., u. L. Quintino: Control of fusion characteristics in pulsed current MIG welding: II-Simple model of fusion characteristics. Metal Constr. 17 (1985), H. 5, S. 314/17.
15) Lenivkin, W. A., u.a.: Technologische Eigenschaften des Schweißlichtbogens in Schutzgasen (russisch). Maschinostroenie, Moskau 1989.
[16] Knoch, R.:Schweißdaten für das MAG-Schweißen. Bericht SLV Miinchen/Carl Cloos.
17) Mayendorf, N., u. R. Nitzsche: Die Temperatur von Zusatzwerkstoffen beim MIG- und MAG- Schweißen. ZIS-Mirt. 25 (1983), H. 3, S. 213/20.
18) Dilthey, U., u. R. Killing: Beitrag zur Berechnung der Wärmeeinbringung beim Metall-Schutzgasschweißen mit Impulslichtbogen. Schw. Schn. 39 (1987), H. 10, S. 495/97.
19) Ondrejcek, P., u.a.: Statistische Spannungsanalyse beim Schweiaen unter 80% Argon 20% coz Schutzgas. ZIS-Mitt. 28 (1986), H. 5, S. 490/98.
20) Choo, R. R. T. C., u.a.: Modelling of High-CurTent Arcs Emphasis on Free Surface Phenomena in the Weld Pool. Wdg. Joumal 69 (1990), H. 9, S. 346/61.
21) Knoch, R.: Schweißkennwerte für das MAG-Schweißen. DVS-Bericht, Band 91. DVS-Verlag, Disseldorf 1985.
22) Dilthey, U., u.a.: Numerische Simulation des Metall-Aktivgasschweißprozesses.Schw. Schn. 45(1993), HZ. 3, S. 148/53.
23) DIN EN25817 „Lichtbogenschweißverbindungen an Stahl; Richtlinie für die Bewertungsgruppen von Unregelmäßigkeiten" (Ausgabe September 1992)
24) Boswort, M.R.: Effective Heat Input in Pulsed Current GMAW with Solid Wire Electrodes. Welding Journal, 1991, No.s, p. 111-117.